Lapine CD133+CD34+ endothelial progenitor cells for musculoskeletal research in preclinical animal trials

Hitesh Chopra
Faculty of Dentistry, The University of Hong Kong.
Yuanyuan Han
Faculty of Dentistry, The University of Hong Kong.
Chengfei Zhang
Faculty of Dentistry, The University of Hong Kong.
Edmond Ho Nang Pow (ehnpow@hku.hk)
Faculty of Dentistry, The University of Hong Kong. https://orcid.org/0000-0003-2640-8437

Research

Keywords: Endothelial progenitor cells, Blood, VEGFR-2, CD34, ULEX, AcLDL

Posted Date: June 22nd, 2020

DOI: https://doi.org/10.21203/rs.3.rs-37026/v1

Lapine $CD133^{+}CD34^{+}$ endothelial progenitor cells for musculoskeletal research in preclinical animal trials

Chopra H[1], Han Yuanyuan[2,] Zhang CF[3], Pow EHN[4]*

1. Chopra H (Dr. Hitesh Chopra) – *Author and Principal investigator*

B.D.S, M.D.S., Ph.D. Student

Department of Restorative Dental Sciences,

Faculty of Dentistry,

The University of Hong Kong.

Email: u3002631@connect.hku.hk

Mob.:+852 9515 9467

2. Han Yuanyuan (Dr. Han Yuanyuan),

B.D.S, M.D.S., Ph.D. student,

Department of Restorative Dental Sciences,

Faculty of Dentistry,

The University of Hong Kong.

Email: u3006886@connect.hku.hk

Mob.: +852 5513 4565

3. Zhang CF (Prof. Cheng Fei Zhang),

D.D.S., Ph.D.

Clinical Professor

Department of Restorative Dental Sciences,

Faculty of Dentistry,

The University of Hong Kong.

Email: zhangcf@hku.hk

Tel.: +852- 28590371

4. Pow EHN (Dr. Edmond Ho Nang Pow) – Corresponding author

B.D.S, M.D.S., Ph.D., M.R.A.C.D.S., F.R.A.C.D.S., F.H.K.A.M. (Dental Surgery), F.C.D.S.H.K. (Prosthodontics).

Clinical Associate Professor

Department of Restorative Dental Sciences,

Faculty of Dentistry,

The University of Hong Kong.

Email: ehnpow@hku.hk

Tel.: +852- 28590309

***Corresponding Author**

3/F, The Prince Philip Dental Hospital, 34 Hospital Road, Sai Ying Pun, Hong Kong

Email: ehnpow@hku.hk

Abstract

Background

Validated animal models form the cornerstone of *in vivo* clinical trials. Rabbits, for instance, have been widely used in musculoskeletal research, but there is a lack of knowledge regarding endothelial progenitor cells (EPCs) obtained from their peripheral blood (PB). Further, there is an ambiguity regarding the origin of EPCs in blood. The present study aimed to isolate and compare rabbit EPCs with human EPCs and explore the origin of EPCs in PB.

Methods

Mononuclear cells (MNCs) were isolated from the PB of rabbits and humans by density centrifugation. Different parameters, such as seeding density, type of medium, and technique (Depletion v/s Hills technique) were standardized for the emergence of EPCs. Homogenous rEPCs and hEPCs were isolated by double sorting with fluorescence-activated cell sorting (FACS) using CD34CD133 or CD34VEGFR-2 antibody. Expanded $CD34^{+}CD133^{+}$ EPCs from both rabbits and humans were compared using growth curve, acetylated low-density lipoprotein (acLDL) uptake, lectin binding, flow cytometry, immunofluorescence (IF), tubulogenic assay, and NO production.

Results

Initial seeding density of MNCs at 1×10^{6} cells/cm^{2} with EGM-2MV supplemented with 5% FBS using depletion technique (40% as compared to 20% by Hill's technique) was found to be optimal for culturing EPCs. Further, depletion technique yielded cobblestone EPCs in 28% of rabbit samples as compared to 40% of human blood specimens in three different patterns blood-island like cell culture (central lEPCs and peripheral early EPCs), biphasic EPCs (early EPCs and late EPCs), and *de novo* EPCs (late EPCs only). Homogenous rEPCs and hEPCs were

sorted using $CD34^{+}CD133^{+}$ and $CD34^{+}VEGFR\text{-}2^{+}$ antibody. Further, with FACS analysis, $rCD34^{+}CD133^{+}$EPCs were found to be one third (3%) as compared to human $CD34^{+}CD133^{+}$EPCs (12%). These $CD34^{+}CD133^{+}$ rEPCs/hEPCs were double-positive for acLDL uptake, ULEX binding, CD34, CD309, and CD31; whereas negative for CD133, CD14 and CD45. Also, EPCs from both species demonstrated functional characterization.

Conclusions

$rCD34^{+}CD133^{+}$EPCs in general, were mostly similar to human $CD34^{+}CD133^{+}$EPCs in proliferative potential, functional characterization, and phenotypic identity. However, the rEPCs appeared to be larger, expressed higher phenotype expression, higher NO production, and had a significantly thicker junctional area, tube thickness, and longer tubule length *($P<0.05$).*

Keyword: Endothelial progenitor cells, Blood, VEGFR-2, CD34, ULEX, AcLDL

wordcount: 344

Background

Blood has been the center stage for assessing the pathophysiological functions of the human body for many decades. The reporting of EPCs has triggered a mammoth investigation by clinical researchers globally [1]. Encouraging results in human and experimental trials expanded the role of EPCs in physiological and pathophysiological angiogenesis for therapeutic use in various diseases such as diabetes [2], cancer [3], cardiovascular disorders [4]. Concomitant with their potential for vascularization, EPCs have also been used extensively in tissue engineering. Tissue-engineered grafts pre-vascularized with EPCs can minimize cell death and improve integration that can enhance graft survival [5].

EPCs, a type of mononuclear cells with low density in blood, have been described based upon their isolation methods [1, 6, 7]. Correspondingly, phylogenetic origin and phenotype of these putative endothelial cells have shrouded a laudable controversy. Asahara et al. described "Blood-island" like morphologic pattern in the emergence of these EPCs and broadly classified them into early EPCs (eEPCs) and late EPCs (lEPCs) [1, 8-10]. eEPCs and lEPCs are also known as circulating angiogenic cells (CACs) [11] and endothelial outgrowth cells (ECFCs) [12] or endothelial colony-forming cells (ECFCs) [13], respectively. Although both share some standard features like the expression of CD31, CD34, DiIacLDL (1,1′-dioctadecyl-3,3,3′,3′-tetramethyindocarbocyanide-labeled low-density lipoprotein) uptake, and UEA-1 lectin (Ulex Europaeus Agglutinin-1) binding, they also have distinct attributes concerning their morphology, proliferative potential, tubulogenic potential *in vitro* and mechanism of neovascularization *in vivo* [8-12, 14-18].

In translational research, EPCs were isolated and characterized from various animals such as rats [19], rhesus monkeys [20], broiler chickens [21], baboons [22], and pigs [23]. Although in 35% of the musculoskeletal research [24] rabbits were used, rEPCs were only isolated and

partially characterized as a prerequisite for their use in the experiments [25, 26]. Studies comparing EPCs of rabbits with the human were lacking.

To our knowledge, this is the first study to characterize rabbit EPCs in the full spectrum. Further, we hypothesized that the rEPCs were similar to hEPCs regarding the proliferative potential, functional characterization, and the expression of surface markers. Hence, rEPCs could provide an excellent research model for translational research in medicine. Additionally, an in-depth understanding of the origin of EPC will be beneficial to researchers and the scientific community.

Methods

Blood sampling

Rabbit blood sampling

The committee on the use of live animals in teaching and research (CULATR: 3558-15) of The University of Hong Kong approved 25 healthy New Zealand white male rabbits (≈ 9-month-old and weighing ≈ 4 kg) for the study. Under topical anesthesia, 30-100 ml of blood was extracted from the marginal ear vein of the rabbit [27, 28], followed by heparinization with heparin sodium (150 IU/ml; Leo pharma, Denmark). The first 5ml of collected blood contaminated with mature endothelial cells (ECs) was discarded. After selection, sample collection, and initial processing in the laboratory animal unit (LAU, The University of Hong Kong, Hong Kong), the samples were transferred to the centralized research laboratory (Faculty of Dentistry, Prince Phillip Dental Hospital, Hong Kong) in a cold storage box for subsequent experimentation.

Human blood sampling

The study was approved by the Institutional review board (IRB: UW 18-222) of The University of Hong Kong. Following written informed consent, 30 ml of blood was withdrawn by venepuncture technique from 10 randomly selected adults of the Faculty of dentistry, Prince Philip Dental Hospital, The University of Hong Kong). The exclusion criteria included subjects with any prevailing medical conditions and smoking habits. Also, 5 ml of first-pass blood was discarded to prevent contamination by the mature endothelial cells.

Isolation of mononuclear cells (MNCs)

Rabbit mononuclear cells (MNCs) were isolated by density gradient centrifugation using dual Histopaque (Histopaque 11191 & Histopaque 18031, Sigma-Aldrich, Shanghai, China)

according to the manufacturer instructions [29]. Briefly, undiluted blood was carefully layered on Histopaque 11191 and Histopaque 1803 [Ratio: 1(Undiluted blood): 0.5(Histopaque 11191) + 0.5(Histopaque 1803)]. The layered column was centrifuged at 700×g for 30 mins. Subsequently, the buffy coat containing rabbit MNCs at the interface was carefully withdrawn.

On the other hand, Ficoll-Paque Premium (GE Healthcare Biosciences, PA, USA) was used according to the manufacturer's instructions to isolate MNCs from human blood. Briefly, the blood was first diluted with PBS (1:1 ratio). The diluted blood (4 ml) was then carefully layered over Ficoll-Paque Premium (3 ml), followed by centrifugation at 400 × g for 40 mins. These MNCs (buffy coat) at the interface were then carefully withdrawn and processed further.

Culturing of rabbit and human MNCs

The MNCs from the rabbit and human PB were washed twice with PBS at 100×g to remove separating media and platelets. These MNCs were then plated at three different densities of 0.5×10^6 cells, 1×10^6 cells/cm^2 and 5×10^6 cells/cm^2 (n=3) in the custom coated six-well plates (2.5 μg/cm^{2,} human plasma fibronectin, Gibco; ThermoFisher Scientific, MA, USA) [1] in the medium X [EGM-2 or EGM-2MV; Lonza, Basel, Switzerland)]. The MNCs were cultured according to the depletion technique or the re-plating technique (Hills technique) in either EGM-2 or EGM-2MV supplemented with an additional 8%, and 5% fetal bovine serum (FBS) respectively. acLDL uptake and lectin binding were used to test the efficacy of the protocols or the type of medium in EPCs yield. After the first medium change, the cells were carefully monitored under a microscope every day for 14 days.

Isolation of homogenous EPCs by FACS

After testing appropriate culture conditions, second and subsequent media was changed accordingly. At 70-80 % confluency, EPCs were passaged to obtain a sufficient number for

double sorting ($CD34^+CD133^+$ or $CD34^+VEGFR\text{-}2^+$) with FACS. The protocol was described later in this section, along with the analysis of surface markers.

Culturing and expansion of sorted $CD34^+CD133^+$ or $CD34^+VEGFR\text{-}2^+$EPCs

Both sorted $CD34^+CD133^+$ or $CD34^+$ $VEGFR\text{-}2^+$ EPCs were cultured, expanded, and evaluated for their characteristic morphology by microscopic examination. The EPCs which maintained their morphology over subsequent passaging were used for analysis and comparison.

Growth curve

The proliferative potential of EPCs was determined by the CCK-8 assay (Sigma-Aldrich). In brief, $rCD34^+CD133^+$EPCs and $hCD34^+CD133^+$EPCs (r/h $CD34^+CD133^+$EPCs) at P5 passage were seeded in 96-well plates at a density of 1000 cells/well and cultured in medium X at 37°C in a humidified atmosphere containing 5% CO_2. The Optical density (OD) was measured every two days for two weeks. On the day of evaluation, medium X was replaced by a phenol red-free culture medium containing 5% FBS, 1% P/S (working medium), and 10μL of CCK-8. The plates were measured for absorbance at 460 nm (OD) by a microplate reader after incubating for 2 hrs at 37°C. The experiment was performed in triplicate, with each set having three wells. The negative control consisted of the working medium and 10 μL of the CCK-8 solution. The OD of both experimental groups at each time point was calculated by subtracting the mean of negative control values from the values of the experimental group at that time point. The population doubling time (PDT) in the logarithmic growth phase of both r/h $CD34^+CD133^+$EPCs was also calculated.

Flow cytometry

After obtaining the homogeneous $CD34^+CD133^+$/$CD34^+VEGFR\text{-}2^+$ EPCs by FACs, the percentage of cell surface markers, such as CD34, CD133, CD31, VEGFR-2, CD45, and CD14

were evaluated by expanding the respective cell population. 1.5-3.0×10^6 cells and 0.5-1.0×10^6 cells were used for sorting and analysis, respectively. The cells were simultaneously blocked (0.1% BSA) and incubated with the antibody (Supplementary Table 1) for 45 mins in an icebox with gentle shaking. After washing twice with cold PBS for 5 mins, the sample was further incubated with the secondary or conjugated antibody for 45 mins and washed. For isolation, dual antibody CD34/CD133 or CD34/VEGFR-2 were used, whereas, for quantitative analysis of surface markers, the single stem cell marker was used. Regarding the control groups, unstained cells served as the negative control, whereas cells with isotype of the corresponding antibody served as an isotype control. The isotype control was also incubated for 30-45 mins followed by washing thrice for 5 mins in PBS. All samples were strained with a 70 μm filter to obtain singlets. BD SORP (BD Biosciences) and BD LSR Fortessa (BD Biosciences) were used for sorting and analysis, respectively, using the markers described above. Minimum 1% of cells were collected after sorting, whereas a minimum of 20,000 events were recorded for analysis. The data were analyzed by FlowJo Version 10.0 (FlowJo, LLC, Ash- land, OR, USA).

Immunofluorescence (IF)

r/h $CD34^+CD133^+$EPCs at P4-P6 were seeded in 6-well plates at a density of 15000 cells/well where three wells were used as treatment group while the other three wells were used as an isotype control group. The experiment was performed in triplicate. At 60-70 % confluency cells were washed twice with PBS for 2 mins and fixed in cold 4% PFA for 30 mins. The cells were then blocked with 1% bovine serum albumin (BSA) (Sigma-Aldrich) for 1 hr, followed by overnight incubation with antibodies. For secondary antibody (CD34), two additional steps were performed, first washing the primary antibody twice for 5 mins and secondly, incubating with the secondary antibody for another 45 mins. The cells were then counterstained with DAPI (Sigma-Aldrich) and analyzed with a fluorescent microscope.

Functional characterization

Tubulogenic assay

r/h $CD34^+CD133^+$EPCs at P5 were evaluated for their ability to form tube formation by Matrigel (BD Biosciences) assay. Briefly, 200 µl of thawed (1.5 ml, overnight at 4°C) Matrigel was carefully added (avoid any air bubbles) into six wells (n=3) of prechilled 96 well plate and incubated at 37°C for 30 mins. 2×10^5 cells/ml single-cell suspension of EPCs was prepared in EGM-2MV. 100 µl of cell suspension was added to the gel gently without disturbing the gel surface. The plate was incubated at 37°C with 5% CO_2 and left undisturbed for 1 hr, after which tube formation was examined every 5 hrs beginning at 1 hr till 25 hrs under an inverted microscope at 4X. Eight randomly selected areas from both the Fig.s of r/h $CD34^+CD133^+$EPCs were chosen and quantitatively analyzed.

acLDL uptake and lectin binding

Expanded r/h $CD34^+CD133^+$EPCs at P5 were assessed for acLDL uptake [30] and lectin binding [31]. Briefly, first ECs at day 7 (P0) (for qualitative confirmation of ECs in EGM-2 or EGM-2MV) or expanded r/h $CD34^+CD133^+$ (P5) EPCs were incubated with DiI-ac-LDL (Molecular Probes, Invitrogen, Carlsbad, CA, USA) at 2.4 µg/ml for 4 hrs in the medium at 37°C. These EPCs were then washed three times with PBS and fixed with 4% paraformaldehyde (PFA) for 30 mins at room temperature. Subsequently, the ECs were counterstained with 200 µL of mouse anti-human UEA-1 antibody-conjugated with fluorescein isothiocyanate (FITC) (Sigma, St. Louis, USA) at 4°C for 1 hr and then washed three times with PBS. The fluorescent images were captured under a laser scanning confocal microscope (Olympus IX81, Japan). DAPI (4′,6-diamidino-2-phenylindole) at a concentration of 0.1 µg/ml was used as negative control.

eNOS assay

Nitric oxide (NO) production by endothelial nitric oxide synthase (eNOS) in r/h $CD34^{+}CD133^{+}$EPCs was assessed by using 4,5 diamino-fluorescein diacetate **(**DAF 2-DA) [32]. Briefly, EPCs were cultured overnight in a black clear-bottom 96-well plate without serum and growth factors. The next day, medium in 96-well plates was replaced by the reaction mixture of 200 µl containing DAF-2 DA, 0.1mM L arginine, and reaction buffer with β NADPH (induction group) or without β NADPH (positive control and blank respectively). After incubating for 2 hrs at room temperature, fluorescence was measured (Ex/Em 490/520 nm) using a fluorimeter (VersaFluor Fluorometer, BioRad). Experiments were performed in quadruplicate in which rEPCs and hEPCs were seeded together with control, blank, and experimental groups together in 96 well plates. Relative fluorescence intensity (RFI) for each group at different concentrations was calculated by subtracting the values of the blank group from treatment group (AFI, Actual fluorescence intensity) as well as the control group followed by dividing the AFI treatment group by AFI control group.

Statistical Analysis

The growth of r/h $CD34^{+}CD133^{+}$EPCs was evaluated by analyzing the difference in the mean OD by 2-way repeated-measures ANOVA for testing the difference in mean growth between two groups at the same time point as well as between different time points within the same group. Similarly, in eNOS assay, the difference in the mean relative fluorescence intensity was analyzed by 2-way repeated-measures ANOVA for testing the difference in mean RFI between 2 groups (rEPCs and hEPCs) at the same concentrations as well as between different concentrations within the same group. The Bonferroni correction was used for adjusting the pairwise comparison. The above tests were performed as the two-sided tests at the 0.05 significance level using IBM SPSS Statistics 24 (IBM Corp. Armonk, NY, USA).

Results

Rabbit and human blood sampling

Both the rabbit and human blood were successfully withdrawn. However, extracting rabbit blood was technically challenging and required extended time as compared to removing human blood (Fig. 1.A). After centrifugation, the buffy coat of MNCs (Fig. 1.B.1) was carefully pipetted and transferred into sterile tubes (Fig. 1.B.2). However, while withdrawing the MNCs, if any blood contamination occurred, the pipettes were discarded immediately.

Culturing of MNCs and emergence of EPCs

We found that MNCs at 1.0×10^6 cells/cm^2 yielded optimal results. No ECs were obtained at 0.5×10^6 cells, whereas at 5.0×10^6 cells/cm^2, cell clumping, and cell death occurred (Fig. 2.A). In our preliminary experiments, the Hills technique was found to be ineffective and was only successful in 20% of cases (1/5 blood samples) tested, whereas the depletion technique yielded EPCs in 40% of cases (2/5 blood samples). Both EGM-2 and EGM-2MV gave positive results, but EPCs in EGM-2MV emerged earlier and greater in number as observed microscopically (Fig. 1.B). acLDL uptake and lectin binding confirmed the emergence of EPCs (Fig. 3). In the depletion technique, the first medium was changed on the fourth day for both rabbit and human MNC's culture. From day 5 to day 7, 28% (7/25) of rabbit blood samples (rBS) and 40% (4/10) of human blood samples (hBS) yielded cobblestone EPCs in three different patterns; blood island-like cell clusters, biphasic EPCs, and *de novo* EPCs (Fig. 3). Spindle-shaped cells (Fig. 3A) occurred in the rest of the cases (referred to as eEPCs) and died within 1-2 weeks, whereas blood island-like cell clusters (Fig. 3B) and biphasic EPCs (Fig. 3C) contained a mixture of eEPCs and lEPCs (ECFCs). *De novo* EPCs (Fig. 3D) were essentially the lEPCs (ECFCs) only.

Isolation, culturing and expansion of EPCs

Both rEPCs and hEPCs were successfully sorted with $CD34^+CD133^+$/$CD34^+VEGFR\text{-}2^+$ using FACS. However, the percentage of $CD34^+CD133^+$ rEPCs was one-third (3%) (Fig. 5A) as compared to the hEPCs (12%). On the other hand, the percentage of $CD34^+VEGFR\text{-}2^+$ EPCs was significantly higher in both rabbits (39.7%), and humans (43.4%) as compared to $CD34^+CD133^+$ sorted EPCs.

rEPCs and hEPCs were successfully cultured and expanded. However, after P7/P8, $CD34^+VEGFR\text{-}2^+$EPCs began to lose their characteristic cobblestone appearance and proliferative potential, whereas both of the properties were intact in $CD34^+CD133^+$EPCs. Therefore, for subsequent analysis and comparison, $CD34^+CD133^+$EPCs were used. It was also observed that rEPCs appeared to be larger than hEPCs (Fig. 5B).

Growth curve

The growth curve (Fig. 5C, Table 2) revealed a statistically significant difference in overall time points ($P<0.05$) as wells as between time points ($P<0.05$) and groups ($P<0.05$). Significant growth was observed from day 2 to day 8 ($P<0.05$). PDT for rEPCS was 21.18 hrs, whereas, for hEPCs, it was 20.01 hrs. Overall, both rEPCs and hEPCs revealed a similar growth pattern.

Flow cytometry and immunofluorescence

FACS analysis demonstrated similar expression for r/h $CD34^+CD133^+$EPCs. Both rEPCs and hEPCs were strongly positive for CD34, CD31, and VEGFR-2. However, rEPCs had a higher percentage of these markers as compared to hEPCs (Fig. 6). CD45, a pan leukocytic cell marker, and CD14, a monocytic lineage marker, were absent in both cell populations. Further, it was noteworthy that expanded $CD34^+CD133^+$ lacks $CD133^+$ expression (Fig. 6). IF results substantiated the findings from FACS analysis. Both rEPCs and hEPCs were positive for CD34, CD31, and VEGFR-2, whereas negative for CD133, CD45, and CD14 (Fig. 7).

Functional characterization

Tubulogenic assay

The tubulogenic assay revealed that r/h $CD34^+CD133^+$EPCS formed a characteristic tubule on Matrigel. In general, the tubules in hEPCs were more uniform and hence could sustain for a comparatively longer time as compared to rEPCs (Fig. 8A). However, quantitative analysis of selected areas revealed that r$CD34^+CD133^+$EPCS had a significantly thicker junctional area, tube thickness, and longer tubule length ($P<0.05$) at 5 hrs as well as 8 hrs as compared to h$CD34^+CD133^+$EPCs (Fig. 8B).

acLDL uptake and lectin binding

Both r/h $CD34^+CD133^+$EPCs demonstrated specific acLDL binding and uptake of UEA-1 with no observable difference observed between rEPCs or hEPCs (Fig. 9A).

eNOS assay

A significantly increased NO production in both r/h $CD34^+CD133^+$EPCs was observed with 0.5μM of β NADPH. Further, at different concentrations of β NADPH, it was found that the rEPCs released higher but statistically insignificant ($P>0.05$) NO as compared to hEPCs (Fig. 9B, Table 3).

Discussion

As blood is the source of EPCs, the foremost question was how much blood could be withdrawn from an animal/human? A rule of thumb is the 10 percent-10 percent rule. Accordingly, safe sampling volume is 10 percent of the total blood volume, which is estimated to be 10 percent of the animal's body weight. In other words, safe sampling volume is 1% of total body weight [27]. Therefore, 30 ml of blood was withdrawn from the rabbit of approximately 3 kg, whereas in humans, a standard 30 ml of blood was collected. It was also observed that the greater the amount of blood, the higher were the chances of isolating EPCs because only 0.05-0.2 lEPCs/ml are present in the blood [33]. Various studies had also collected a similar amount of blood (30-100 ml) for isolating EPCs [9, 13, 34, 35].

If lEPCs are difficult to isolate, the next question was, how many cells should be seeded/cm^2 of the culture ware? There were two essential considerations; firstly, efficient MNC recovery, and secondly, appropriate seeding density. MNCs were isolated by various techniques, such as; magnetic bead separation, FACS, and density gradient centrifugation. However, density gradient centrifugation with Ficoll-Paque is the most widely used technique. For isolation of hMNCs, we adhered to Ficoll-Paque Premium. However, for isolation rMNCs, we used a dual Histopaque technique because the density of rabbit MNCs is higher as compared to humans, and that could give the highest and purest mononuclear cell recovery [29]. As the density of solution increases, the osmotic shock is reduced in Histopaque as compared to Ficoll-Paque, thereby reducing cell death and increasing cell recovery [29].

We also found that only 1.0×10^6 MNCs/cm^2 yielded EPCs. In another study, 1.5×10^6 cells/cm^2 was used as the initial seeding density. However, researchers did not test the minimum cell concentration required for EPCs isolation [34]. Another important consideration is whether the

coating of culture ware can improve the efficiency of EPCs isolation? We used custom made fibronectin-coated dishes instead of collagen because morpho-differentiation and proliferation of EPCs were found to be significantly higher in fibronectin-coated dishes/flasks as compared to the collagen-coated dishes [1].

Culture media is decisive for defining cell characteristics. In literature, there is a discrepancy in the type of media used for the isolation of EPCs from PBMNCs [9, 35-37]. In our study, we found that EPCs emerged on day six in EGM-2MV as compared to day 9 in EGM-2. Further, uptake of acLDL and UEA-1 uptake was higher in EGM-2MV as compared to EGM-2, indicating that they were more metabolically active in EGM-2MV than EGM-2. Our results were in correspondence with another study in which EGM-2MV increased colony count, cell differentiation, adhesion, tubulogenic potential, and NO production of EPCs cells, particularly lEPCs [38].

The EPCs have been traditionally classified into eEPCs and lEPCs based on the appearance in the culture media and their phenotypic expression (CD34, CD 45, CD14, CD31, VEGFR-2, and CD133). Both early and late EPCs express CD34. CD31/PECAM-1 (platelet endothelial cell adhesion molecule) is strongly expressed in lEPC but weakly expressed (focal expression) in eEPC [9, 14, 39]. On the other hand, Flk-1 (VEGFR-2 in mouse, or KDR human homolog of VEGFR-2), is expressed weakly in eEPCs but strongly expressed in lEPCs [9, 10, 14, 15, 39]. Regarding CD45 and CD14, these can be found only on eEPCs but not on lEPCs [9, 14, 16]. CD133, a member of 5 transmembrane glycoproteins, is expressed on both hematopoietic stem and progenitor cells (HSCs). It is a transitional marker found variably on circulating endothelial cells, eEPCs, and lEPCs, but not on mature and differentiated endothelial cells [40].

In this study, we were able to successfully isolate $CD34^{+}CD133^{+}$ from the heterogenous EPC population and expand EPCs. However, when the expanded r/h$CD34^{+}CD133^{+}$EPCs

populations were further analyzed, CD133 was found to absent from both cell populations. The results confirmed that CD133 is an early marker, and when sorted $CD34^{+}CD133^{+}$ were expanded, they transformed into mature cells and lost their CD133 expression. The results were supported by another study where the authors found that EPCs differentiated into mature cells having cobblestone appearance (lEPCs), which were $CD34^{+}$ VEGRF-2^{+} but $CD133^{-}$ [17]. In another study, researchers were able to generate endothelial cells (lEPCs) from $CD133^{+}$ cells [18]. In sharp contrast, some researchers were neither able to detect VEGFR-2 transcripts in $CD133^{+}$cells nor generate lEPCs from $CD133^{+}$cells. They hypothesized that $CD34^{+}$VEGFR-$2^{+}CD133^{-}$cells within the heterogenous $CD34^{+}$fraction might be the origin of the lEPCs [16].

The tubulogenic assay is a specific assay for endothelial cells. In the present study, characteristic tubules were formed on Matrigel. eEPCs failed to create a tube-like structure, whereas lEPCs did, indicating an inferior endothelial function of eEPCs *in vitro.* lEPCs expressed FLK-1 which might be responsible for VEGF mediated tube formation [9]. In the current study, both $rCD34^{+}CD133^{+}$EPCs and $hCD34^{+}CD133^{+}$EPCs did form a tubular network, as seen on microscopic examination, but the junctional area, tubule thickness, and length of tubules were larger in rEPCs as compared to hEPCs. It might explain why rabbits are called as potential healers as compared to humans.

The selectivity of endothelial cells can also be demonstrated by the ability to bind with DiI acLDL [30] and UEA-1 uptake [31]. The distinct advantages of Dil-ac-LDL assay include its reproducibility, uniform labeling without any permeabilization or fixing, non-sensitivity to trypsinization, and no effect on the growth rate of endothelial cells. On the other hand, lectin binds specifically to L-fructose residues on endothelial cells [41]. Both types of EPCs bind with acLDL and uptake UEA-1, but the level of binding and uptake in eEPCs was less as compared to lEPCs suggesting higher metabolic activity in lEPCs [9]. Our results revealed the

same that the uptake and binding intensity in the primary culture of EPCs were significantly less than that in homogenous and sorted $CD34^{+}CD133^{+}$EPCs.

The detection of the release of NO is another functional assay to characterize EPCs. NO is generated *in vivo* through the conversion of L-arginine to L-citrulline by NO synthase (NOS). It mediates many physiological and pathophysiological processes in the human body [42]. DAF-2DA is a highly sensitive, specific, and a membrane-permeable fluorescent probe where DAF-2 reacts rapidly and irreversibly in solution with NO and NO-derived reactive species in a concentration-dependent manner to produce the highly fluorescent product triazolofluorescein (DAF-2T) [32]. We measured the RFI of $CD34^{+}CD133^{+}$EPCs by using β NADPH as it is one of the co-factors in the pathways of NO production [43]. We found no significant difference in the production of NO in either human or rabbit EPCs.

The other exciting finding in the present study, apart from the similarities between rEPCs and hEPCs, was the emergence of two distinct colonies of EPCs. Classically, EPCs were suggested to grow from blood-island cell-like clusters that have round cells in the center and spindle shape cells in the periphery. The spindle-shaped cells are traditionally classified as eEPCs because they appear earlier in culture, whereas lEPCs, emerged later in the culture. We found two other patterns apart from blood-island like structures, biphasic EPCs, and *de novo* late EPCs. In "biphasic EPCs", lEPCs did not need to emerge after eEPCs. In fact, both eEPCs and lEPCs were simultaneously growing together, and because early EPCs have a short life span, they eventually die, allowing lEPCs to proliferate and increase in number. The corresponding presence of both eEPCs and lEPCs in our study, proved previous studies stipulating lEPCs arise from cells other than eEPCs [9, 15, 35]. On the other hand, "*de novo* lEPCs" are termed so because these lEPCs emerge without any significant eEPCs in a culture. The said pattern is reminiscent of endothelial colony-forming cells (ECFCs) described in various studies [13, 33, 44]. Therefore, the appearance of biphasic EPCs and *de novo* lEPCs suggested that some lEPCs

might emerge from cells different from eEPCs and they do not form a typical colony. In the rest of the cultures, spindle-shaped cells were observed, and even after culturing over an extended period, these were not able to give cobblestone appearance, a hallmark of true EPCs. We concluded that these are early EPCs and the appearance of these cells was an indicator of failure to isolate true EPCs.

To explain the above results, an overview of studies on EPCs and monocytes is imperative. Initial studies revealed that eEPCs are a heterogeneous population of $CD14^+$ and $CD14^-$ and lEPCs originate from $CD14^-$ cells [8, 9, 15]. A decade later, gene expression, microarray, and proteomic analysis confirmed that eEPCs have a monocytic phenotype [39]. Further, eEPCs were found to be positive for CD16, where $CD16^+CD14^-$ population generated more CFU-Hill colonies than $CD16^+CD14^+$. However, only these two populations were able to produce eEPCs but not the $CD16^-CD14^+$ or $CD16^-CD14^-$ [45]. Parallelly, monocytes were classified into classical monocytes ($CD14^{++}$, $CD16^-$), intermediate monocytes ($CD14^{++}$, $CD16^+$), and non-classical monocytes ($CD14^-$, $CD16^+$) [46]. Additionally, it was also found out that some cells from intermediate monocytes expressed several surface markers associated with pro-angiogenesis, including endoglin (ENG), TEK tyrosine kinase (Tie2, CD202b) and KDR (VEGFR-2) [47]. If we correlate the two parallel themes of studies in the hematopoietic domain, early EPCs might probably arise from intermediate monocytes, whereas lEPCS are true endothelial cells. This hypothesis can be supported by various studies in which endothelial cells could transform the phenotype and function of monocytes [48, 49].

There were several limitations in the present study. We compared only $CD34^+CD133^+$population because these cells can be passaged to higher generations, unlike $CD34^+VEGFR\text{-}2^+$ cells. Another limitation was the unavailability of anti CD133 and VEGFR-2 rabbit antibodies in the market. The development of anti CD133 and VEGFR-2 rabbit

antibodies might shed more light on rabbit EPCs and its analogy to human EPCs. Additionally, we did not evaluate the neovascularization potential of rCD34^{+}CD133^{+} by an *in vivo* study because our next research goal will be to determine the potential of rabbit periodontal ligament cells (rPDLCs) [50] with rCD34^{+}CD133^{+} in neoosteogenesis in an irradiated rabbit model, in which rPDLCs will function as bone-forming cells and rCD34^{+}CD133^{+} will take part in neovascularization.

Conclusions

$CD34^+CD133^+$ EPCs were isolated, expanded, and characterized from human and rabbit peripheral blood. In general, although $rCD34^+CD133^+$EPCs were similar to $hCD34^+CD133^+$EPCs in proliferative potential, functional characterization, and phenotypic identity. However, the rEPCs appeared to be larger, expressed higher phenotype expression, higher NO production, and had a significantly thicker junctional area, tubule thickness, and longer tubule length.

Abbreviations

EPCs: Endothelial progenitor cells

ECs: Endothelial cells

rEPCs: Rabbit endothelial progenitor cells

hEPCs: Human endothelial progenitor cells

rBS: Rabbit blood sample

hBS: Human blood sample

eEPCs: Early endothelial progenitor cells

lEPCs: Late endothelial progenitor cells

EGM-2: Endothelial growth medium-2

EGM-2 MV: Endothelial growth medium-2 Microvascular

acLDL: Acetylated low-density lipoprotein

UEA-1: Ulex Europaeus Agglutinin- 1

eNOS: Endothelial nitric oxide synthase

DAPI: 4′,6-diamidino-2-phenylindole

FACS: Fluorescence-activated cell sorting

FITC: Fluorescein isothiocyanate

OD: Optical density

VEGFR-2: Vascular endothelial growth factor-2

Declarations

Ethics approval and consent to participate

The isolation and study of rEPCs were approved by the "Committee on the Use of Live Animals in Teaching and Research" [CULATR: 3558-15 (1st amendment-16): EHNP & HC] while the isolation and study of rEPCs from human blood were approved by Institutional Review Board (IRB: UW 18-222, EHNP & HC) of the University of Hong Kong. Written informed consent was obtained from the patients for the study, publication of this report, and any accompanying images.

Consent for publication

Not applicable

Availability of data and materials

The datasets supporting the conclusions of this article are included within the article.

Competing interests

The authors declare that they have no competing interests

Funding

Chopra H was supported through a seed grant no. 201511159105 awarded to Pow EHN and Zhang CF by University Research Grants for "3D cell sheets cultured from endothelial progenitor cells and periodontal ligament stem cells (2016)."

Authors' contributions

H.C., E.H.N.P., and C.F.Z. conceived and designed the experiments. H.C. performed all the experiments except Matrigel assay, which was done by Y.H. H.C. drafted the manuscript while

multipaneled Figures were designed by Y.H. Data analysis, interpretation, and revision of the manuscript was done by H.C., Y.H., E.H.N.P., and C.F.Z. E.H.N.P and C.F.Z provided administrative and financial support. All authors had read and approved the final manuscript.

Acknowledgments

We are thankful to Dr. Mei Ki Hung for human blood sampling. We also appreciate Dr. Dan Zhao (Ph.D. student, Faculty of Dentistry, The University of Hong Kong) and Prof. Jin (Clinical Professor, Periodontology) for helping us with their appointed nurse in human blood collection.

References

1. Asahara T, Murohara T, Sullivan A, Silver M, van der Zee R, Li T, et al. Isolation of putative progenitor endothelial cells for angiogenesis. Science. 1997, 275:964-67.

2. Fadini GP, Sartore S, Agostini C, Avogaro A. Significance of endothelial progenitor cells in subjects with diabetes. Diabetes Care. 2007, 30:1305-13.

3. Mancuso P, Bertolini F. Circulating endothelial cells as biomarkers in clinical oncology. Microvasc Res. 2010, 79:224-28.

4. Dong C, Goldschmidt-Clermont PJ. Endothelial progenitor cells: a promising therapeutic alternative for cardiovascular disease. J Interv Cardiol. 2007, 20:93-99.

5. Rouwkema J, Rivron NC, van Blitterswijk CA. Vascularization in tissue engineering. Trends Biotechnol. 2008, 26:434-41.

6. Hill JM, Zalos G, Halcox JP, Schenke WH, Waclawiw MA, Quyyumi AA, et al. Circulating endothelial progenitor cells, vascular function, and cardiovascular risk. N Engl J Med. 2003, 348:593-600.

7. Ito H, Rovira II, Bloom ML, Takeda K, Ferrans VJ, Quyyumi AA, et al. Endothelial progenitor cells as putative targets for angiostatin. Cancer Res. 1999, 59:5875-77.

8. Gulati R, Jevremovic D, Peterson TE, Chatterjee S, Shah V, Vile RG, et al. Diverse origin and function of cells with endothelial phenotype obtained from adult human blood. Circ Res. 2003, 93:1023-25.

9. Hur J, Yoon CH, Kim HS, Choi JH, Kang HJ, Hwang KK, et al. characterization of two types of endothelial progenitor cells and their different contributions to neovasculogenesis. Arterioscler Thromb Vasc Biol. 2004, 24:288-93.

10. Mukai N, Akahori T, Komaki M, Li Q, Kanayasu-Toyoda T, Ishii-Watabe A, et al. A comparison of the tube forming potentials of early and late endothelial progenitor cells. Exp Cell Res. 2008, 314:430-40.

11. Rehman J, Li J, Orschell CM, March KL. Peripheral blood "endothelial progenitor cells" are derived from monocyte/macrophages and secrete angiogenic growth factors. Circulation. 2003, 107:1164-69.

12. Lin Y, Weisdorf DJ, Solovey A, Hebbel RP. Origins of circulating endothelial cells and endothelial outgrowth from blood. J Clin Invest. 2000, 105:71-77.

13. Ingram DA, Mead LE, Tanaka H, Meade V, Fenoglio A, Mortell K, et al. Identification of a novel hierarchy of endothelial progenitor cells using human peripheral and umbilical cord blood. Blood. 2004, 104:2752-60.

14. Cheng CC, Chang SJ, Chueh YN, Huang TS, Huang PH, Cheng SM, et al. Distinct angiogenesis roles and surface markers of early and late endothelial progenitor cells revealed by functional group analyses. BMC Genomics. 2013, 14:182.

15. Yoon CH, Hur J, Park KW, Kim JH, Lee CS, Oh IY, et al. Synergistic neovascularization by mixed transplantation of early endothelial progenitor cells and late outgrowth endothelial cells: the role of angiogenic cytokines and matrix metalloproteinases. Circulation. 2005, 112:1618-27.

16. Timmermans F, Van Hauwermeiren F, De Smedt M, Raedt R, Plasschaert F, De Buyzere ML, et al. Endothelial outgrowth cells are not derived from CD133(+) cells or CD45(+) hematopoietic precursors. Arterioscler Thromb Vasc Biol. 2007, 27:1572-79.

17. Peichev M, Naiyer AJ, Pereira D, Zhu Z, Lane WJ, Williams M, et al. Expression of VEGFR-2 and AC133 by circulating human CD34(+) cells identifies a population of functional endothelial precursors. Blood. 2000, 95:952-58.

18. Gehling UM, Ergun S, Schumacher U, Wagener C, Pantel K, Otte M, et al. In vitro differentiation of endothelial cells from AC133-positive progenitor cells. Blood. 2000, 95:3106-12.

19. Thomas RA, Pietrzak DC, Scicchitano MS, Thomas HC, McFarland DC, Frazier KS. Detection and characterization of circulating endothelial progenitor cells in normal rat blood. J Pharmacol Toxicol Methods. 2009, 60:263-74.

20. Sun W, Zheng L, Han P, Kang YJ. Isolation and characterization of endothelial progenitor cells from Rhesus monkeys. Regen Med Res. 2014, 2:5.

21. Bi S, Tan X, Ali SQ, Wei L. Isolation and characterization of peripheral blood-derived endothelial progenitor cells from broiler chickens. Vet J. 2014, 202:396-99.

22. Hinds MT, Ma M, Tran N, Ensley AE, Kladakis SM, Vartanian KB, et al. Potential of baboon endothelial progenitor cells for tissue engineered vascular grafts. J Biomed Mater Res A. 2008, 86:804-12.

23. Avci-Adali M, Nolte A, Simon P, Ziemer G, Wendel HP. Porcine EPCs downregulate stem cell markers and upregulate endothelial maturation markers during in vitro cultivation. J Tissue Eng Regen Med. 2009, 3:512-20.

24. Neyt J, Buckwalter JA, Carroll N. Use of animal models in musculoskeletal research. Iowa orthopaedic j. 1998, 18:118.

25. Amini AR, Laurencin CT, Nukavarapu SP. Differential analysis of peripheral blood- and bone marrow-derived endothelial progenitor cells for enhanced vascularization in bone tissue engineering. J Orthop Res. 2012, 30:1507-15.

26. Lam CF, Liu YC, Hsu JK, Yeh PA, Su TY, Huang CC, et al. Autologous transplantation of endothelial progenitor cells attenuates acute lung injury in rabbits. Anesthesiology. 2008, 108:392-401.

27. McGuill MW, Rowan AN. Biological effects of blood loss: implications for sampling volumes and techniques. ILAR J. 1989, 31:5-20.

28. Parasuraman S, Raveendran R, Kesavan R. Blood sample collection in small laboratory animals. J Pharmacol Pharmacother. 2010, 1:87-93.

29. Feldman DL, Mogelesky TC. Use of Histopaque for Isolating Mononuclear-Cells from Rabbit-Blood. J Immunol Methods. 1987, 102:243-49.

30. Voyta JC, Via DP, Butterfield CE, Zetter BR. Identification and Isolation of Endothelial-Cells Based on Their Increased Uptake of Acetylated-Low Density Lipoprotein. J Cell Biolo. 1984, 99:2034-40.

570 31. Holthofer H, Virtanen I, Kariniemi AL, Hormia M, Linder E, Miettinen A. Ulex europaeus
571 I lectin as a marker for vascular endothelium in human tissues. Lab Invest. 1982, 47:60-
572 66.

573 32. Kojima H, Nakatsubo N, Kikuchi K, Kawahara S, Kirino Y, Nagoshi H, et al. Detection
574 and imaging of nitric oxide with novel fluorescent indicators: diaminofluoresceins. Anal
575 Chem. 1998, 70:2446-53.

576 33. Prater DN, Case J, Ingram DA, Yoder MC. Working hypothesis to redefine endothelial
577 progenitor cells. Leukemia. 2007, 21:1141-9.

578 34. Bueno-Beti C, Novella S, Lazaro-Franco M, Perez-Cremades D, Heras M, Sanchis J, et al.
579 An affordable method to obtain cultured endothelial cells from peripheral blood. J Cell
580 Mol Med. 2013, 17:1475-83.

581 35. Medina RJ, O'Neill CL, Sweeney M, Guduric-Fuchs J, Gardiner TA, Simpson DA, et al.
582 Molecular analysis of endothelial progenitor cell (EPC) subtypes reveals two distinct cell
583 populations with different identities. BMC Med Genomics. 2010, 3:18.

584 36. Kalka C, Masuda H, Takahashi T, Kalka-Moll WM, Silver M, Kearney M, et al.
585 Transplantation of ex vivo expanded endothelial progenitor cells for therapeutic
586 neovascularization. Proc Natl Acad Sci U S A. 2000, 97:3422-27.

587 37. Mai XL, Ma ZL, Sun JH, Ju SH, Ma M, Teng GJ. Assessments of proliferation capacity
588 and viability of New Zealand rabbit peripheral blood endothelial progenitor cells labeled
589 with superparamagnetic particles. Cell Transplant. 2009, 18:171-81.

590 38. Guan XM, Cheng M, Li H, Cui XD, Li X, Wang YL, et al. Biological properties of bone
591 marrow-derived early and late endothelial progenitor cells in different culture media. Mol
592 Med Rep. 2013, 8:1722-28.

593 39. Cheng SM, Chang SJ, Tsai TN, Wu CH, Lin WS, Lin WY, et al. Differential expression
594 of distinct surface markers in early endothelial progenitor cells and monocyte-derived
595 macrophages. Gene Expr. 2013, 16:15-24.

596 40. Chopra H, Hung MK, Kwong DL, Zhang CF, Pow EHN. Insights into Endothelial
597 Progenitor Cells: Origin, Classification, Potentials, and Prospects. Stem Cells
598 International. 2018, 2018:9847015.

599 41. Hormia M, Lehto VP, Virtanen I. Identification of UEA I-binding surface glycoproteins
600 of cultured human endothelial cells. Cell Biol Int Rep. 1983, 7:467-75.

601 42. Murad F. Discovery of some of the biological effects of nitric oxide and its role in cell
602 signaling. Bioscience Reports. 2004, 24:452-74.

603 43. Forstermann U, Sessa WC. Nitric oxide synthases: regulation and function. Euro Heart J.
604 2012, 33:829-37d.

605 44. Yoder MC, Mead LE, Prater D, Krier TR, Mroueh KN, Li F, et al. Redefining endothelial
606 progenitor cells via clonal analysis and hematopoietic stem/progenitor cell principals.
607 Blood. 2007, 109:1801-9.

608 45. Kimura T, Kohno H, Matsuoka Y, Nakatsuka R, Sasaki Y, Fukuhara S, et al. CD16 antigen
609 is a positive marker of peripheral blood-derived early endothelial progenitor cells. Int J
610 Hematol. 2011, 93:123-25.

611 46. Ziegler-Heitbrock L, Ancuta P, Crowe S, Dalod M, Grau V, Hart DN, et al. Nomenclature
612 of monocytes and dendritic cells in blood. Blood. 2010, 116:e74-80.

613 47. Zawada AM, Rogacev KS, Rotter B, Winter P, Marell R-R, Fliser D, et al. SuperSAGE
614 evidence for CD14++CD16+ monocytes as a third monocyte subset. Blood. 2011,
615 118:e50-e61.

616 48. Thomas-Ecker S, Lindecke A, Hatzmann W, Kaltschmidt C, Zanker KS, Dittmar T.
617 Alteration in the gene expression pattern of primary monocytes after adhesion to
618 endothelial cells. Proc Natl Acad Sci U S A. 2007, 104:5539-44.

619 49. Tso C, Rye K-A, Barter P. Phenotypic and functional changes in blood monocytes
620 following adherence to endothelium. PloS one. 2012, 7:e37091-e91.

621 50. Chopra H, Liao C, Zhang CF, Pow EHN. Lapine periodontal ligament stem cells for
622 musculoskeletal research in preclinical animal trials. J Transl Med. 2018, 16:174.

623

Figure legends

Fig. 1. Extract and isolation of MNCs. A. Extraction of blood from 1) Rabbit 2) Human **B.** Isolation of MNCs by density centrifugation 1) Buffy coat formation after density centrifugation at 700×g for 30 mins for rabbit samples and 400×g for 40 mins for human samples 2) Buffy coat was carefully transferred without RBC contamination and re-centrifuged for culturing of acquired MNCs.

Fig. 2. Culturing of EPCs. **A.** Rabbit MNCs were seeded in 3 different densities with representative images taken on day 6 1) 0.5×10^6 cells/cm^2 2) 1.0×10^6 cells/cm^2 3) 5.0×10^6 cells/cm^2 (n=3, 10X, Pixel size: 0.9 µm, Scale bar: 100 µm) **B.** Influence of culture medium. Emergence of rEPCs on day 6 after culturing 1.0×10^6 cells/cm^2 in different mediums. Representative images (n=3, 10X, Pixel size: 0.9 µm, Scale bar: 100 µm) in 1) EGM-2 medium 2) EGM-2MV medium.

Fig. 3. **acLDL binding and UEA-1 uptake.** The emergence of EPCs was confirmed by acLDL binding and UEA-1 uptake assay**.** Rabbit MNCs cultured in EGM-2MV revealed a higher number of EPCs as compared to EGM-2. Representative images of staining of rEPCs with DAPI, UEA-1, acLDL, and merged from the three experiments (n=3, 4X, Pixel size: 2.22 µm, Scale bar: 500 µm).

Fig. 4. **Variations in the emergence of EPCs.** Both rabbit (n=25 rBS) and human MNCs (n=10 hBS) cultured at 1.0×10^6 cells/cm^2 of the 6-well plate in EGM-2MV medium revealed 4 different types of appearance from day 5 - day 7. **A.** Spindle-shaped cells (eEPCs) (n=18 rBS + 6 hBS) **B.** Blood-island like cell clusters (eEPCs at the periphery and central round cells) (n=3 rBS + 2 hBS) **C.** Biphasic EPCs (mixed eEPCs and lEPCs) (n=2 rBS + 1 hBS) **D.** *de novo* lEPCs (ECFCs) (n=2 rBS + 1 hBS) (4X, Pixel size: 2.22 µm, Scale bar: 500 µm**).**

Fig. 5. Isolation and expansion of $CD34^+CD133^+$EPCs. Homogenous r/h $CD34^+CD133^+$EPCs were isolated from the primary culture of EPCs by double sorting with CD34 and CD133 antibody. **A.** Representative scatter plots of r/h $CD34^+CD133^+$EPCs population (n=3). **B.** Microscopic examination of expanded **r**$CD34^+CD133^+$EPCs (60-70% confluency) and **h**$CD34^+CD133^+$EPCs (80-90% confluency) (n=3, 4X, Pixel size: 2.22 μm). **C.** Growth curve of expanded $CD34^+CD133^+$EPCs with statistically significant differences between human and rabbit group on day 2, 4, 6 and 8 ($P<0.05$).

Fig. 6. Flow cytometric analysis of r/h $CD34^+CD133^+$EPCs. The expression of CD34, CD133, CD31, VEGFR-2, CD45, and CD14 surface antigens by r$CD34^+CD133^+$EPCs and h$CD34^+CD133^+$EPCs were quantitatively analysed by flow cytometry. Histograms were representative of at least three separate experiments, each with a minimum of 20,000 events.

Fig. 7. Immunofluorescence assay r/h $CD34^+CD133^+$EPCs.. Both r/h $CD34^+CD133^+$EPCs at P4-P6 were seeded in 6-well plates at a density of 15000 cells/well and qualitatively analyzed at 60-70 % confluency. Representative images of both rEPCs and hEPCs were positive for CD34, CD31, and VEGFR-2, whereas negative for CD133, CD45, and CD14 (n=3, 60X, Pixel size: 0.25 μm, Scale bar: 100 μm).

Fig. 8. Tubulogenic assay. A. Time course of the tubulogenic assay. 100μl of 2×10^4 r/h $CD34^+CD133^+$EPCs/well were seeded in 96-well microplate. Representative images of tube formation in Matrigel at a 5 hr interval up to 25 hrs (n=3, 4X, Pixel size: 2.22 μm, Scale bar: 500 μm). **B. Quantitative analysis of tubule formation**. Mean (μm ±SD) tube thickness, and tubule length, whereas, mean (μm^2 ±SD) junctional area were analyzed in eight randomly selected areas at 5 hrs as well as 10 hrs. The mean surface area of rEPCs was significantly higher than the mean surface area of hEPCs ($P<0.05$) at both 5 hrs and 10 hrs. r$CD34^+CD133^+$

had a significantly thicker junctional area, tubule thickness, and a longer tubule length (P<0.05) as compared to hCD34$^+$CD133$^+$EPCs.

Fig. 9. Other functional characterization essays. A. acLDL binding and UEA-1 uptake. r/h CD34$^+$CD133$^+$EPCs cultured in EGM-2MV demonstrated characteristic acLDL binding and UEA-1 uptake (DAPI was used as a negative control) (n=3, 20X, Pixel size: 0.44 μm, Scale bar: 100 μm). **B. eNOS assay**. DAF 2-DA did not reveal a significant difference (P>0.05) in NO production by r/h CD34$^+$CD133$^+$EPCs after induction with β NADPH.

Figures

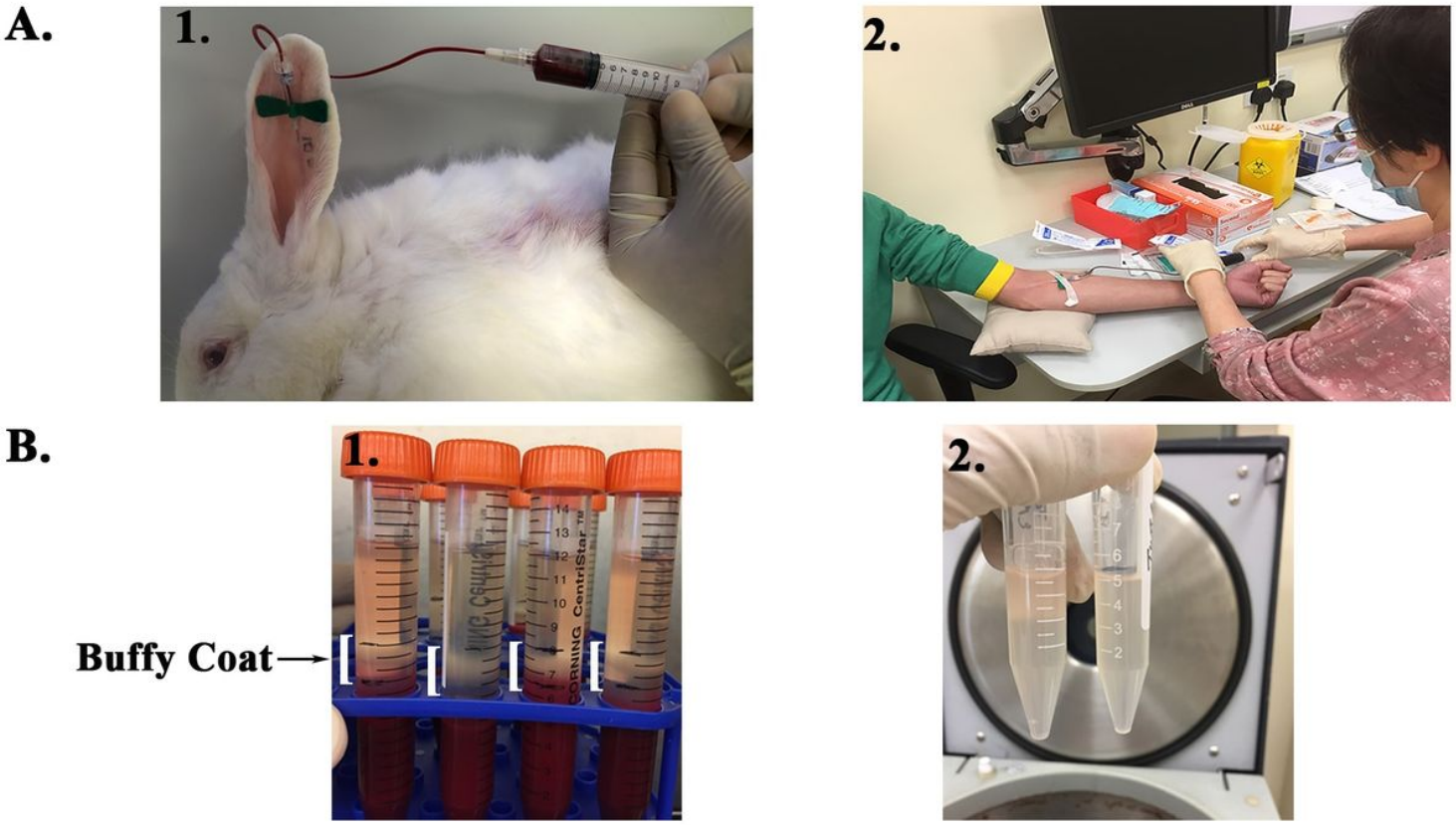

Figure 1

Extract and isolation of MNCs. A. Extraction of blood from 1) Rabbit 2) Human B. Isolation of MNCs by density centrifugation 1) Buffy coat formation after density centrifugation at 700×g for 30 mins for rabbit samples and 400×g for 40 mins for human samples 2) Buffy coat was carefully transferred without RBC contamination and re-centrifuged for culturing of acquired MNCs.

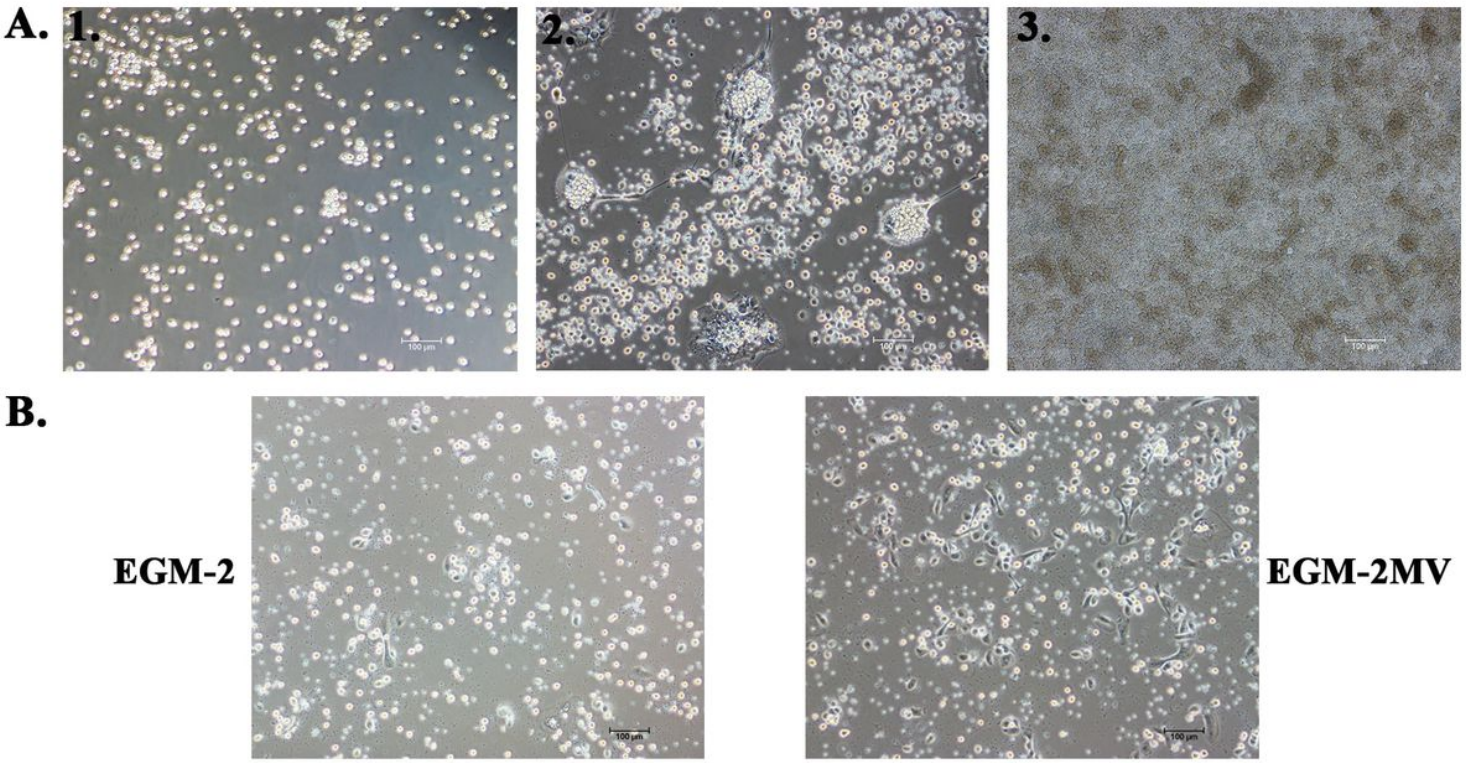

Figure 2

Culturing of EPCs. A. Rabbit MNCs were seeded in 3 different densities with representative images taken on day 6 1) 0.5˝106 cells/cm2 2) 1.0˝106 cells/cm2 3) 5.0˝106 cells/cm2 (n=3, 10X, Pixel size: 0.9 µm, Scale bar: 100 µm) B. Influence of culture medium. Emergence of rEPCs on day 6 after culturing 1.0˝106 cells/cm2 in different mediums. Representative images (n=3, 10X, Pixel size: 0.9 µm, Scale bar: 100 µm) in 1) EGM-2 medium 2) EGM-2MV medium.

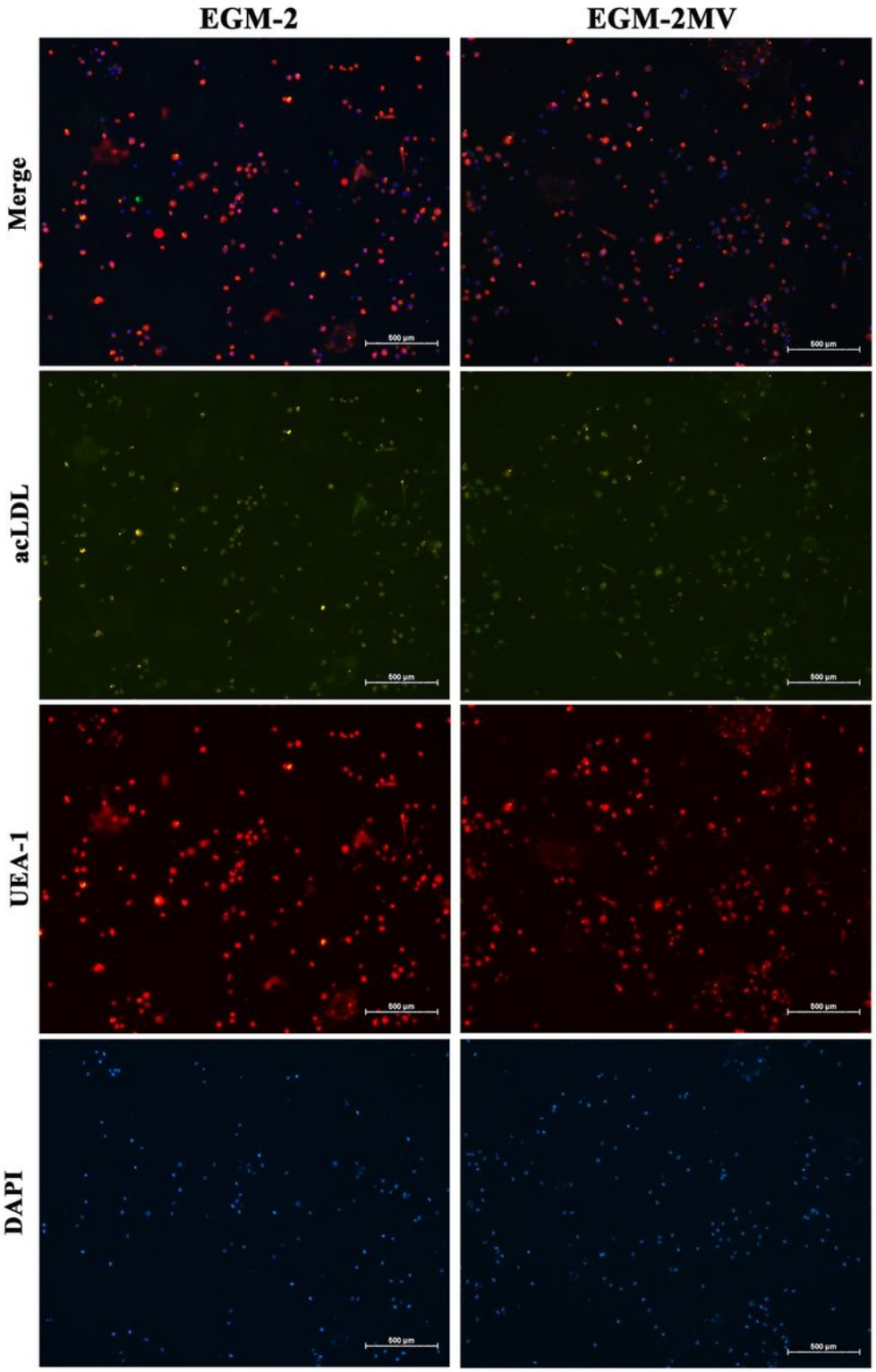

Figure 3

acLDL binding and UEA-1 uptake. The emergence of EPCs was confirmed by acLDL binding and UEA-1 uptake assay. Rabbit MNCs cultured in EGM-2MV revealed a higher number of EPCs as compared to EGM-2. Representative images of staining of rEPCs with DAPI, UEA-1, acLDL, and merged from the three experiments (n=3, 4X, Pixel size: 2.22 µm, Scale bar: 500 µm).

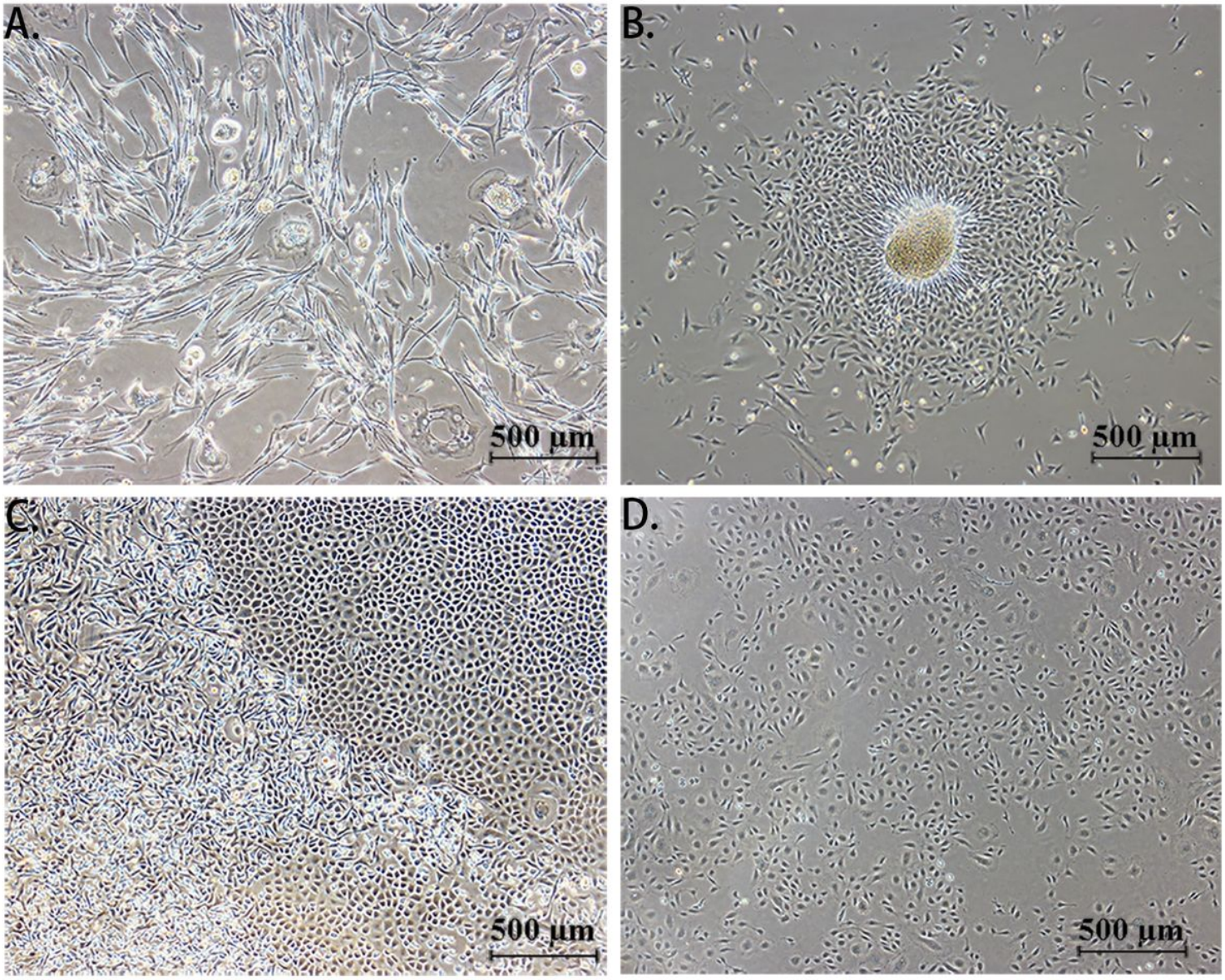

Figure 4

Variations in the emergence of EPCs. Both rabbit (n=25 rBS) and human MNCs (n=10 hBS) cultured at 1.0ᵕ 106 cells/cm2 of the 6-well plate in EGM-2MV medium revealed 4 different types of appearance from day 5 - day 7. A. Spindle-shaped cells (eEPCs) (n=18 rBS + 6 hBS) B. Blood-island like cell clusters (eEPCs at the periphery and central round cells) (n=3 rBS + 2 hBS) C. Biphasic EPCs (mixed eEPCs and lEPCs) (n=2 rBS + 1 hBS) D. de novo lEPCs (ECFCs) (n=2 rBS + 1 hBS) (4X, Pixel size: 2.22 µm, Scale bar: 500 µm).

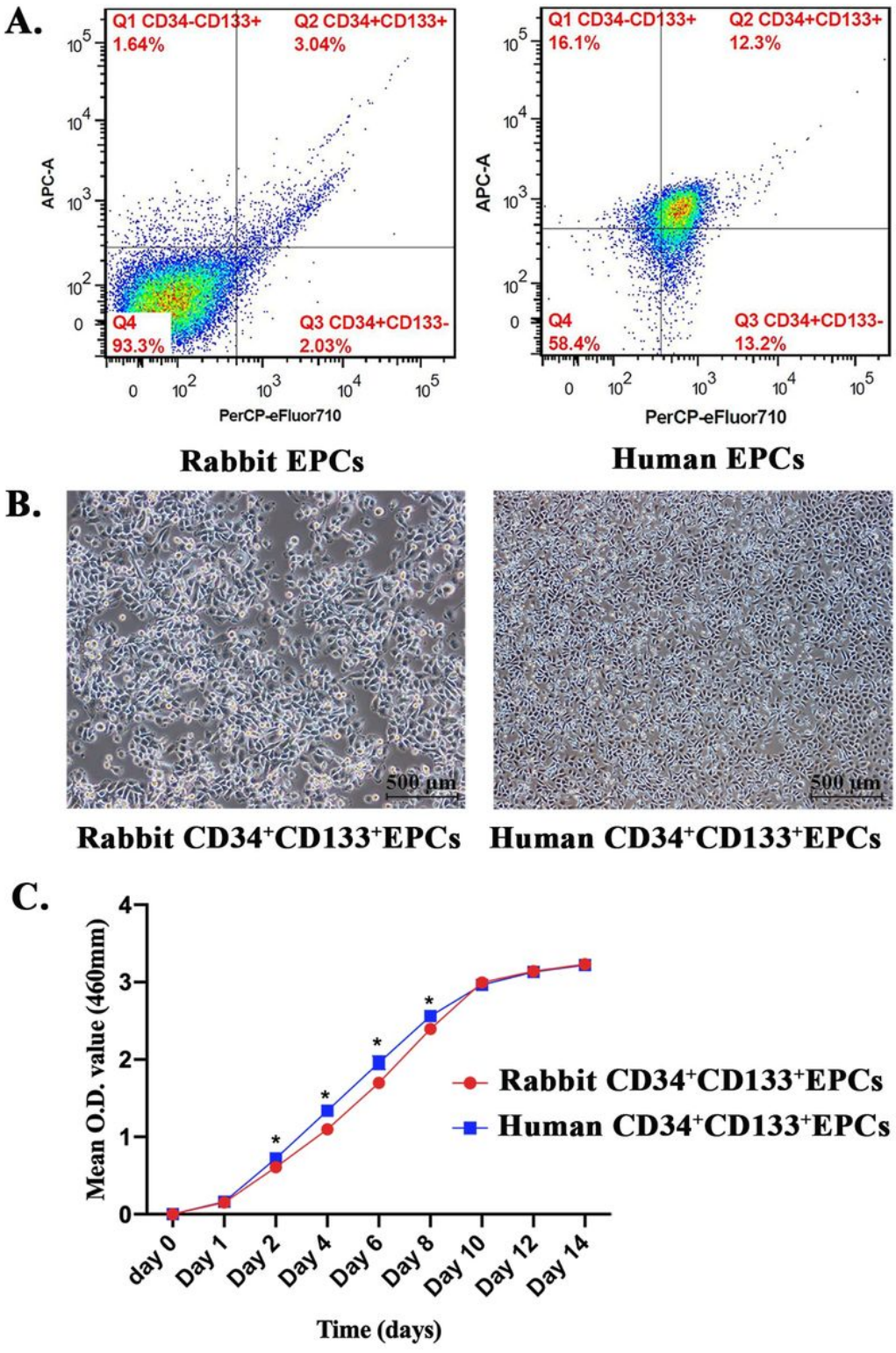

Figure 5

Isolation and expansion of CD34+CD133+EPCs. Homogenous r/h CD34+CD133+EPCs were isolated from the primary culture of EPCs by double sorting with CD34 and CD133 antibody. A. Representative scatter plots of r/h CD34+CD133+EPCs population (n=3). B. Microscopic examination of expanded rCD34+CD133+EPCs (60-70% confluency) and hCD34+CD133+EPCs (80-90% confluency) (n=3, 4X, Pixel

size: 2.22 μm). C. Growth curve of expanded CD34+CD133+EPCs with statistically significant differences between human and rabbit group on day 2, 4, 6 and 8 (P<0.05).

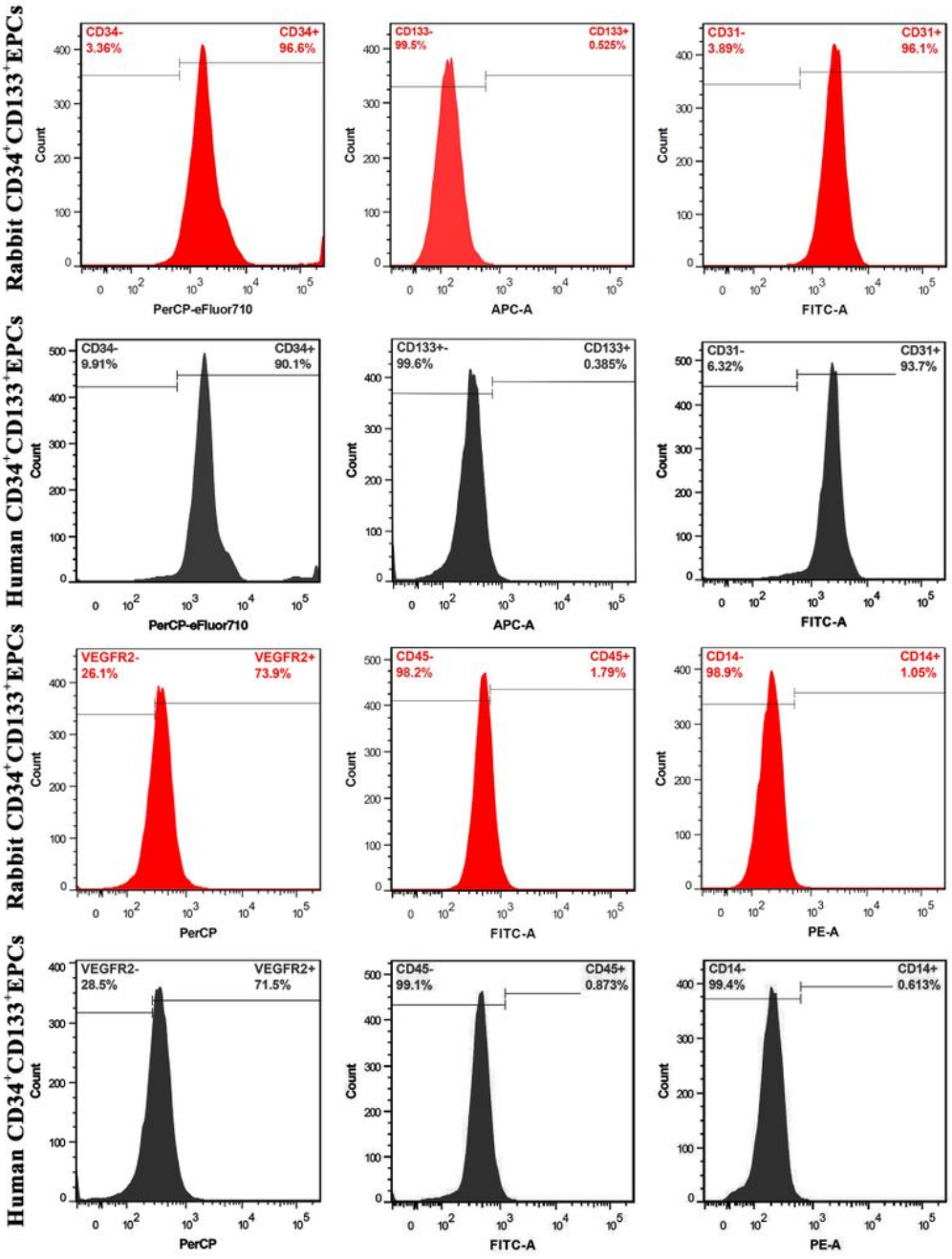

	CD34	CD133	CD31	VEGFR-2	CD45	CD14
rCD34+CD133+EPCs	96.6%	0.525%	96.1%	73.9%	1.79%	1.05%
hCD34+CD133+EPCs	90.1%	0.385%	93.7%	71.5%	0.873%	0.613%

Figure 6

Flow cytometric analysis of r/h CD34+CD133+EPCs. The expression of CD34, CD133, CD31, VEGFR-2, CD45, and CD14 surface antigens by rCD34+CD133+EPCs and hCD34+CD133+EPCs were quantitatively

analysed by flow cytometry. Histograms were representative of at least three separate experiments, each with a minimum of 20,000 events.

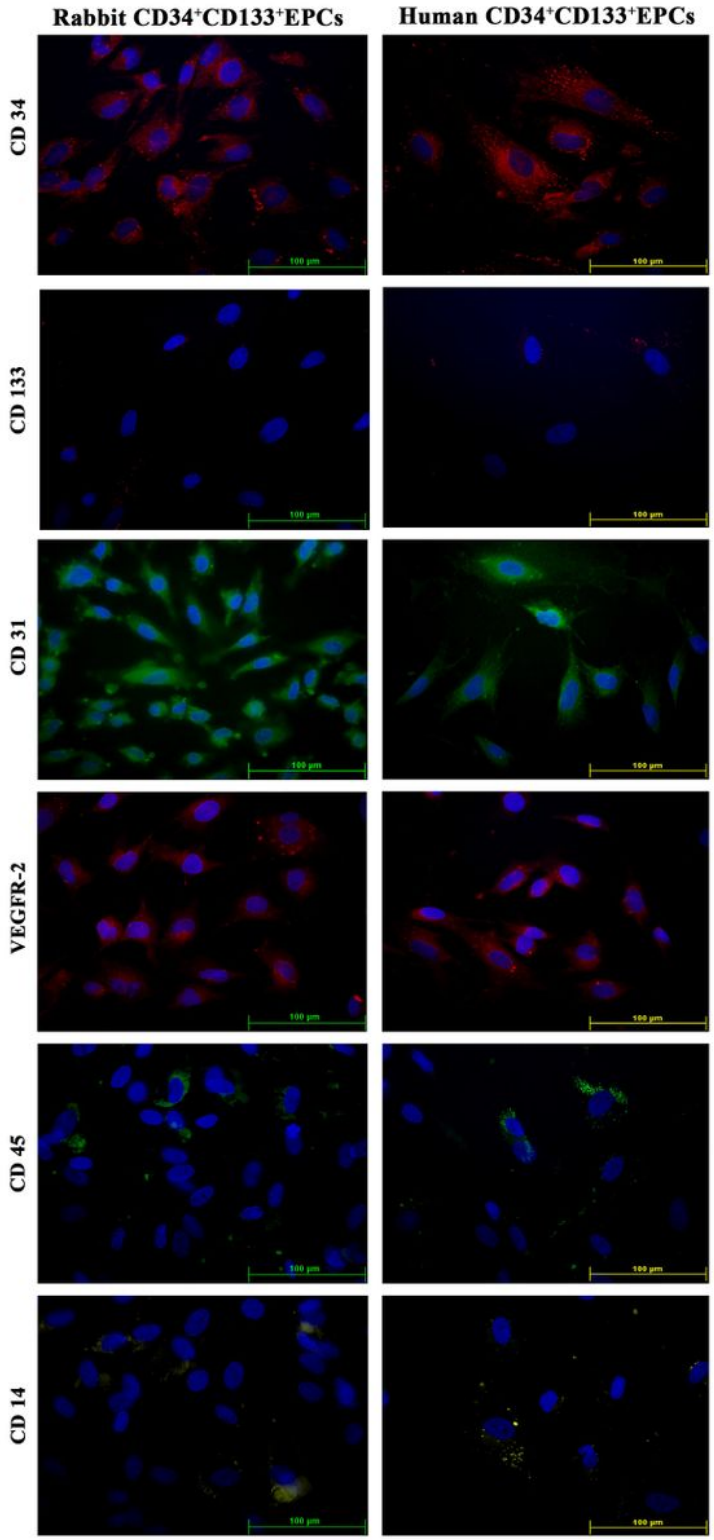

Figure 7

Immunofluorescence assay r/h CD34+CD133+EPCs.. Both r/h CD34+CD133+EPCs at P4-P6 were seeded in 6-well plates at a density of 15000 cells/well and qualitatively analyzed at 60-70 % confluency.

Representative images of both rEPCs and hEPCs were positive for CD34, CD31, and VEGFR-2, whereas negative for CD133, CD45, and CD14 (n=3, 60X, Pixel size: 0.25 μm, Scale bar: 100 μm).

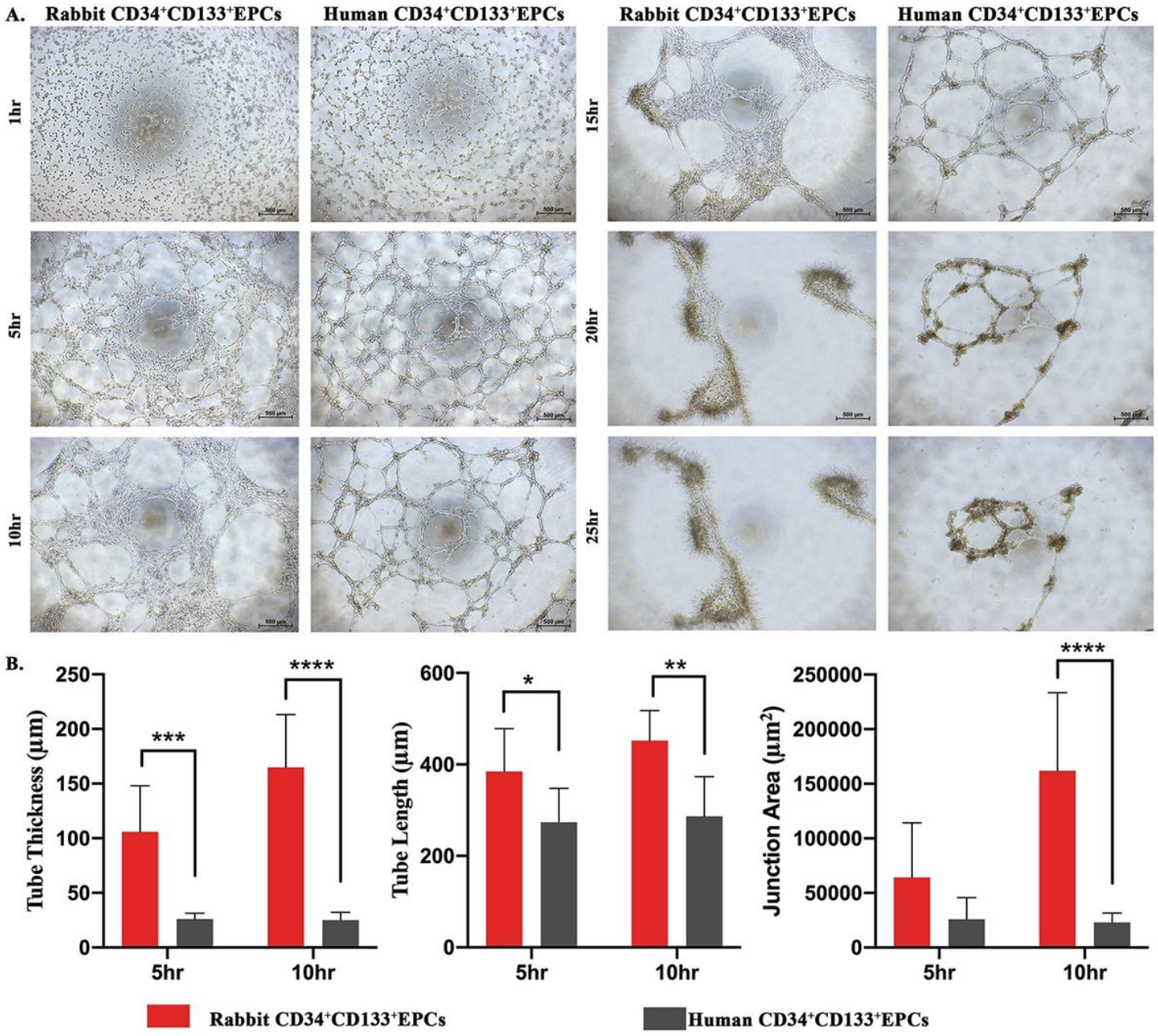

Figure 8

Tubulogenic assay. A. Time course of the tubulogenic assay. 100μl of 2×104 r/h CD34+CD133+EPCs/well were seeded in 96-well microplate. Representative images of tube formation in Matrigel at a 5 hr interval up to 25 hrs (n=3, 4X, Pixel size: 2.22 μm, Scale bar: 500 μm). B. Quantitative analysis of tubule formation. Mean (μm ±SD) tube thickness, and tubule length, whereas, mean (μm2 ±SD) junctional area were analyzed in eight randomly selected areas at 5 hrs as well as 10 hrs. The mean surface area of rEPCs was significantly higher than the mean surface area of hEPCs ($P<0.05$) at both 5

hrs and 10 hrs. rCD34+CD133+ had a significantly thicker junctional area, tubule thickness, and a longer tubule length (P<0.05) as compared to hCD34+CD133+EPCs.

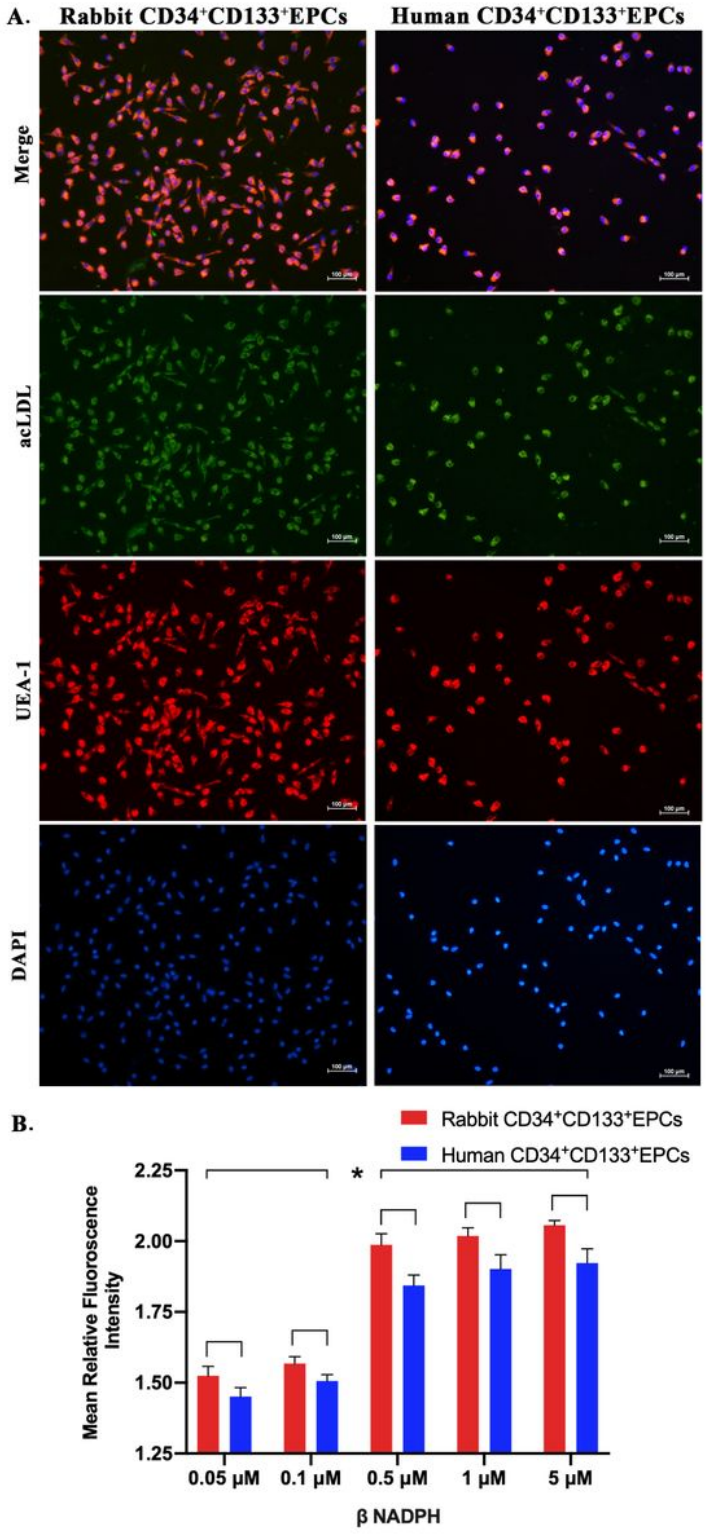

Figure 9

Other functional characterization essays. A. acLDL binding and UEA-1 uptake. r/h CD34+CD133+EPCs cultured in EGM-2MV demonstrated characteristic acLDL binding and UEA-1 uptake (DAPI was used as a negative control) (n=3, 20X, Pixel size: 0.44 μm, Scale bar: 100 μm). B. eNOS assay. DAF 2-DA did not

reveal a significant difference (P>0.05) in NO production by r/h CD34+CD133+EPCs after induction with b NADPH.